batteries

Article

Development of Printed Pouch Film and Flexible Battery

Gyeongseok Oh [1,†], Snigdha Paramita Mantry [2,†], Jae Ho Sim [1], Hyeon Woo Cho [3], Mijin Won [1], Hwamok Park [1], Jiyoung Park [1], Juhwan Lee [1] and Dong Soo Kim [1,*]

[1] Department of Creative Convergence Engineering, Hanbat National University, 125, Dongseodae-ro, Yuseong-gu, Daejeon 34158, Republic of Korea; oks6125@naver.com (G.O.); poseidon96@naver.com (J.H.S.); 0mj00@naver.com (M.W.); phm1078@naver.com (H.P.); ji0_1201@naver.com (J.P.); 11630054@o365.hanbat.ac.kr (J.L.)
[2] Research Institute of Printed Electronics & 3D Printing, Hanbat National University, 125, Dongseodae-ro, Yuseong-gu, Daejeon 34158, Republic of Korea; snigdha.paramita012@gmail.com
[3] Amogreentech Co., Ltd., 17-8 4sandan 7-ro, Jiksan-eup, Seobuk-gu, Cheonan-si 31040, Chungcheongnam-do, Republic of Korea; lpkms@naver.com
* Correspondence: kds671@hanbat.ac.kr; Tel.: +82-42-821-1734; Fax: +82-42-828-8969
† These authors contributed equally to this work.

Abstract: This study investigates the properties of various adhesives and assesses the effects of the coating and drying conditions of aluminum surface treatment agents on adhesion strength and chemical resistance. The adhesion between aluminum and the polymer film is improved through the application of a surface treatment agent to the aluminum surface. This study examines the initial adhesive strength of a manufactured pouch film with respect to the drying temperature and time and evaluates its adhesive strength in the presence of moisture. The results indicate that the residual moisture on the aluminum surface weakens the adhesive strength and significantly affects electrolyte resistance. A noticeable reduction in strength was observed after water spraying, when the drying temperature and time were relatively low during the initial strength measurement. Among the adhesives used for aluminum and CPP lamination, olefin adhesives exhibit less susceptibility to electrolyte effects and have higher adhesive strengths compared to urethane and ester adhesives. Leveraging these characteristics, flexible pouch cells were manufactured and their stability was evaluated. The results confirm that the flexible cells demonstrate excellent stability, exhibiting potential for application in wearable devices.

Keywords: electric vehicle; secondary battery; pouch film; R2R coating and lamination; manufacturing process; flexible battery

Citation: Oh, G.; Mantry, S.P.; Sim, J.H.; Cho, H.W.; Won, M.; Park, H.; Park, J.; Lee, J.; Kim, D.S. Development of Printed Pouch Film and Flexible Battery. *Batteries* **2024**, *10*, 244. https://doi.org/10.3390/batteries10070244

Academic Editor: Johan E. ten Elshof

Received: 9 March 2024
Revised: 24 June 2024
Accepted: 28 June 2024
Published: 8 July 2024

1. Introduction

Secondary batteries can be reused by charging after each use and have economic and environmental benefits [1,2]. Secondary batteries consist of an electrolyte, a positive-electrode active material, negative-electrode active material, separator, and an external casing [3]. Currently, such batteries are used in various appliances such as mobile electronic devices, electric vehicles, energy storage equipment, robots, drones, electric bicycles, and toys [4–6]. These products have become essential items in everyday life. However, recent incidents involving the explosion of lithium-ion batteries have highlighted the importance of pouch films, which act as external casings in maintaining the stability of secondary batteries. The aforementioned positive-electrode active material, negative-electrode active material, separator, and electrolyte have already reached high levels of technological development. However, the source and core technologies related to secondary-battery pouch films are owned by a small number of Japanese firms. The core technologies need to manufacture external materials to ensure formability, chemical resistance, heat-seal strength, and insulation. Among these qualities, chemical resistance is particularly important. The electrolyte is a secondary-battery component that exhibits high permittivity and strong

polarity [7,8], and can form strong acids via side reactions [9–11]. Therefore, chemically resistant surface treatment agents and adhesives are necessary. Equations (1)–(4) depict the process by which hydrofluoric acid is formed by additional reactions between trace amounts of water [8,12] and the electrolyte (Equations (1)–(3)) as well as the process by which aluminum is corroded by the created hydrofluoric acid (Equation (4)), as follows:

$$LIPF_6 \rightarrow LiF + PF_5 \quad (1)$$

$$PF_5 + H_2O \rightarrow 2HF + POF_3 \quad (2)$$

$$POF_3 + H_2O \rightarrow HF + POF_2(OH) \quad (3)$$

$$6HF + 2Al \rightarrow 2AlF_3 + 3H_2 \quad (4)$$

The conventional pouch-film manufacturing technology uses simple adhesion to manufacture food packaging, but the industrial pouch films used in secondary batteries must be highly reliable and maintain their physical properties when exposed to strong chemicals. The number of users who prefer electric vehicles has increased notably, owing to strict regulations on fossil-fuel vehicles due to current environmental issues. Electric vehicle production volumes are rapidly increasing every year. Secondary batteries are key electric vehicle components that must have a guaranteed lifespan of at least 10 years. Their stability must also be ensured under harsh conditions, such as collisions and vibrations, because it directly affects the survival of vehicle passengers. A external material of the secondary battery is a key component that safely protects the high-performance battery cells and determines the lifespan of the battery. Pouch films for secondary batteries, which are multilayer films made of metal foil (aluminum) and polymer film, are examples of such external casing materials [13]. Interlayer adhesion is the most important aspect of multilayer film manufacturing. Methods for facilitating adhesion between heterogenous materials either use materials of the same category or modify material surfaces in an activated state. Multilayer films, such as secondary-battery pouch films, are components that create adhesion between heterogenous materials such as polar metal materials and nonpolar polymer films. Surface treatment materials also require high corrosion resistance and adhesion, therefore, it is necessary to optimize the coating and drying conditions of surface treatment agents.

Various surface treatment agents and pretreatment methods influence the adhesion properties and corrosion performance of epoxy coatings on aluminum alloys. The key surface treatment agents and pretreatment methods include hexafluorozirconic-acid, polyacrylic-acid (PAA), polyacrylamide (PAM) blends, and chromate/phosphate conversion coatings (CPCC). Hexafluorozirconic acid is used as part of the pretreatment formulations. Polyacrylic acid (PAA) is another key component used, in pretreatment formulations interacting with aluminum oxide and other components, to influence the adhesion properties of the coatings. PAM enhances corrosion resistance in combination with PAA and hexafluorozirconic-acid but does not significantly increase adhesion strength. The traditional CPCC was used as a benchmark for comparison with the novel pretreatment formulations [14]. The combination of hexafluorozirconic-acid, PAA, and PAM in the pretreatment formulations played a crucial role in influencing the adhesion strength and corrosion performance of the epoxy coatings on aluminum substrates [15]. These surface treatment agents and pretreatment methods are used for improving the durability and protective properties of coatings on aluminum alloys.

Flexible batteries are a crucial component in the development of bendable electronic devices. Shi et al. and Nishide et al. discussed several significant works conducted for the widespread adoption of flexible batteries in the next generation of electronic devices [16,17]. Taberna et al. explored the use of nanostructured inorganic materials and investigated their potential application in flexible batteries. These materials offer increased rates of electron and counterion transport, making them suitable for bendable lithium-ion batteries [18]. Song et al. investigated radical polymer batteries, which exhibit reversible

one-electron redox reactions with fast kinetics, enabling rapid charging, burst power generation, and flexibility in battery design [19]. Miller et al. focused on the development of organic electrode-active materials with redox-active groups, aiming to increase the overall redox capacity of batteries and facilitate charge storage and transport in flexible battery configurations [20].

This study manufactured a pouch film, by varying the surface treatment agent's temperature and time conditions and changing the adhesive, in order to improve the adhesive strength and chemical resistance of the electric vehicle secondary-battery external pouch. It also examined the differences in adhesive strength and chemical resistance under various conditions. Figure 1a presents the structure of an aluminum and CPP film in an external pouch film of a pouch-type secondary battery; Figure 1b presents the R2R direct-gravure coating and lamination equipment used in the pouch manufacturing process.

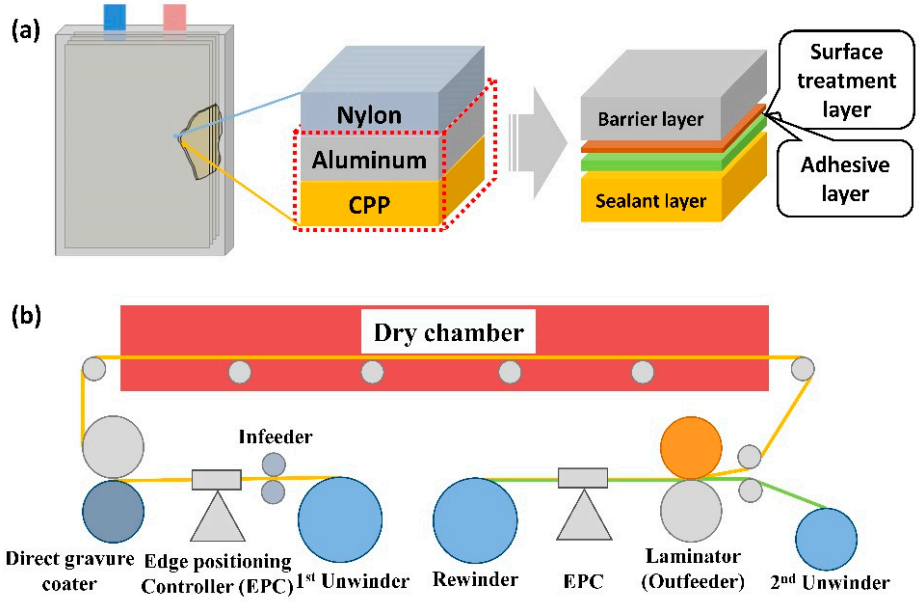

Figure 1. (**a**) Structure of aluminum and CPP film in the external pouch film of a pouch-type secondary battery; and (**b**) diagram of the R2R direct-gravure coating and lamination equipment used in the pouch manufacturing process.

This study evaluated the performance of pouch films manufactured via the above process, and then used a pouch film that had passed stability tests to manufacture a flexible battery cell. The stability of the manufactured flexible cell was confirmed by performing a 3000-cycle bending test. The results suggest that the cell could be used in flexible wearable devices.

2. Experimental Methods

2.1. Preparation of Pouch Film

For the experiments, we prepared a phosphate chromate (trivalent) surface coating agent (Hix1, Why-Chem Co., Seoul, Korea), polyurethane adhesive, polyester adhesive, polyolefin adhesive, and untreated aluminum foil (AA8021) with a thickness of 40 µm. The matte aluminum surface was treated with phosphate chromate (trivalent) and allowed to dry. Then, the aforementioned polyurethane adhesive was applied and allowed to dry. Lamination was then performed with a nylon film to manufacture a nylon–aluminum laminate film. In the experiments, pilot R2R direct-gravure coating and lamination equipment was used to perform the coating, drying, and lamination of the surface treatment agent and adhesives. The surface treatment agent was used to coat the opposite sides of the nylon–aluminum laminate using a 250-lines-per-inch gravure. The aluminum was dried at 80–160 °C for 60 s, and additional drying was performed for 2 h in an electric oven, if necessary. The coated aluminum was coated with various adhesive substances

and then laminated with the aforementioned CPP film at a rate of 300 mm/s. The laminated pouch film was then aged in an oven at 55 °C for three days. Fourier-transform infrared spectroscopy (FT-IR) and thermogravimetric analysis (TGA, TGA/DSC1/1600 LF, Mettler Toledo, Columbus, OH, USA) were used to analyze the properties of the surface treatment agent that coated the aluminum according to the drying conditions. In addition, a scanning electron microscope (SEM) was used to verify the adhesion of the adhesive to the aluminum.

2.2. Pouch Film Performance Test

A tensile strength tester (Authonic AGS-X 500 N, Shimadzu Scientific Korea Corporation, Seoul, Korea) was used to check the adhesive strength between the aluminum and CPP film in the pouch films manufactured under each of the conditions, as presented in Figure 2. In the tensile strength tests, the pouch films were cut into 15 mm × 100 mm pieces, and strength was measured using a 180° delamination test method with measurements at a rate of 300 mm/min.

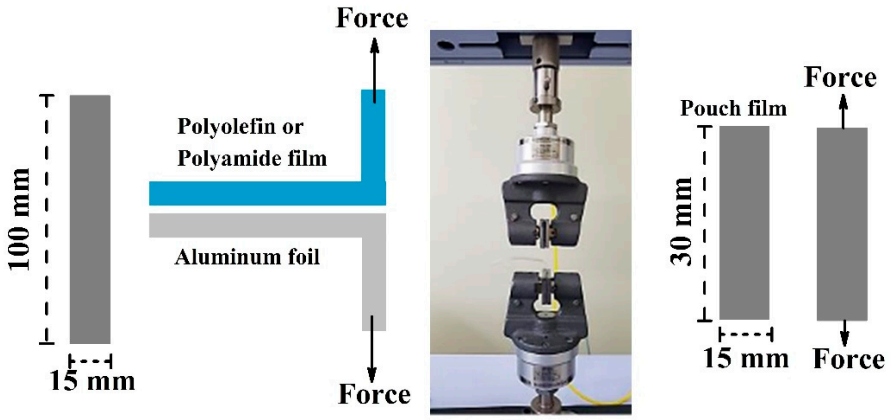

Figure 2. Schematic measurement of tensile and adhesive strengths.

In the electrolyte tests and chemical resistance experiments shown in Figure 3, urethane (A310, Mitsui Chemicals, Tokyo, Japan), ester (Vylon200, Toyobo Korea Co., Ltd., Seoul, Korea), and olefin (Hy-Chem, Hix 2, HI-CHEM Co., Ltd., Seoul, Korea) adhesives were used. To test the chemical resistance of the adhesives, the electrolyte used in the batteries (EC:DEC:DMC = 1:1:1, LiPF 61 M) [21] was added to each type of adhesive, and the changes in the adhesives' weights and appearances over time were examined. In the experiments on the electrolyte resistance of the pouch films created using the various adhesives, the aluminum foil and CPP lamination samples were immersed in the electrolyte, and the aluminum and CPP film's changes in adhesive strength over time at 85 °C were examined.

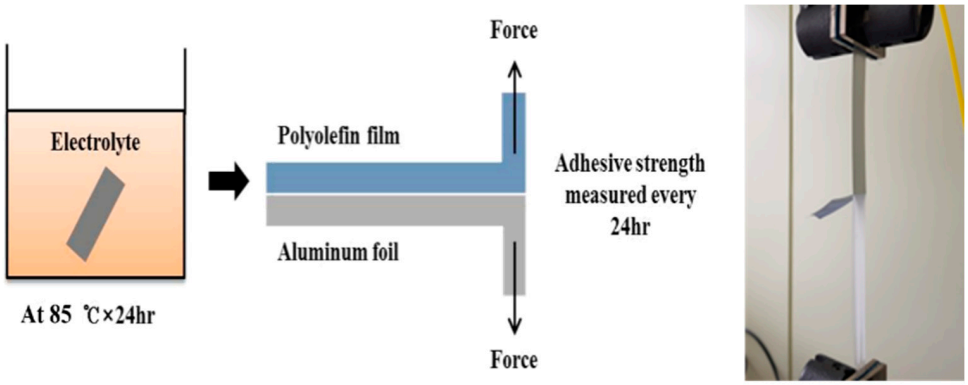

Figure 3. Schematic of electrolyte resistance test.

2.3. Fabrication of Flexible Battery

Dr. Cho at Amogreentech used the pouch films created in the experiments above to manufacture flexible cells that could be used in wearable devices. An LCO base was used as the negative-electrode material, an artificial graphite base was used as the positive-electrode material, PE (20 μm) was used as the separator, and an $LiPF_6$ base was used as the electrolyte. Manufactured flexible cells (Series 4000, Maccor, Tulsa, OK, USA) were used in charging and discharging tests in a 5 V, 5 A environment. An insulation tester (ST 520, Hioki, Seoul, Korea) was used to measure the insulation resistance and a battery tester (BT562, Hioki, Japan) was used to perform the voltage and AC−IR measurements. A U−bending tester (Yuasa System Co., Ltd., Okayama, Japan) was used to perform bending tests and evaluate cell performance.

3. Results and Discussion

3.1. Preparation of Pouch Film

Aluminum surface coating is generally performed to enhance the corrosion resistance and adhesive strength between aluminum and the film. In the experiments, the phosphate–chromate method was used, and a pilot R2R direct-gravure coating device was used to coat the aluminum foil surface. Generally, a natural oxide film forms on the surface of untreated aluminum. This natural oxide film-coating layer is amorphous and consists of aluminum oxide or hydroxide [22]. The surface exhibits weak corrosion resistance. Therefore, it requires chemical coating to increase the corrosion resistance and adhesion. In the experiments, various aluminum foil chemical-coating treatment conditions and different adhesives were used to manufacture pouches, and the differences in adhesive strength and chemical resistance were examined.

Figure 4a shows the FTIR spectra of bare aluminum, aluminum with adsorbed moisture, and aluminum heat-treated for 2 h at 160 °C. The peak area of the wide region around 3000–3600 cm^{-1} decreased in the following order: aluminum that was dried for 2 h at 160 °C, bare aluminum, and aluminum with adsorbed water. The presence of this peak is attributed to moisture or hydrates [23], and suggests that residual moisture is important in these samples. Figure 4b shows the FTIR results of the samples in which the aluminum surface was coated with the water-based surface treatment agent and heat-treated for 60 s at 80 °C, 60 s at 120 °C, and 2 h at 160 °C. The intensity of the peaks varied according to the heat treatment temperature and time. The wide peak observed around 3260 cm^{-1} exhibits a decreasing trend as the drying temperature and time increased. This trend seems to be associated with the residual moisture present on the surface-treated aluminum. Upon increasing the drying temperature and drying time, the peaks at 1452 and 1335 cm^{-1} are reduced, and the peak at 1184 cm^{-1} is enlarged. This is because the phosphate–chromate species changes into phosphate–chromate compounds after moisture and solvents are sufficiently removed through drying. The results in Figure 2 were confirmed by the TGA results. TGA is the ideal compositional method for detecting volatile substances (moisture, solvents, etc.), polymers, carbon black, carbon fiber, ash, and filler content. Figure 5 shows the TGA results of bare aluminum, and the aluminum samples heat-treated for 60 s at 120 °C and 2 h at 160 °C.

The reduction in weight that occurred in the 50−250 °C range as the temperature increased from 50 to 450 °C is caused by moisture or hydrates on the aluminum surface and the residual moisture after coating with the surface treatment agent when heat treatments were performed at different temperatures.

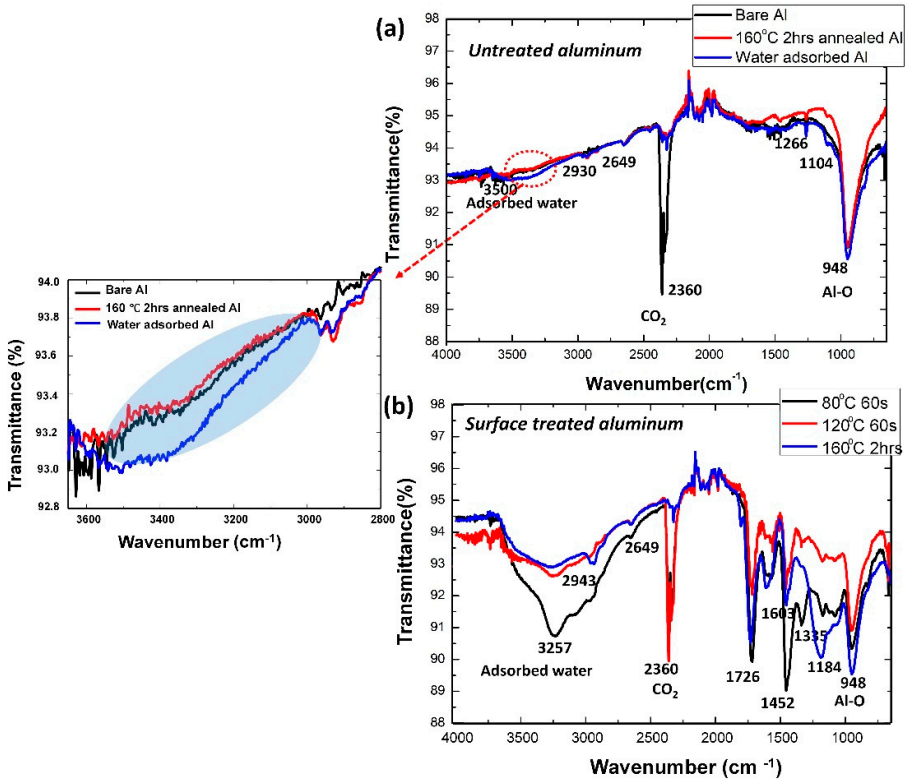

Figure 4. (**a**) FTIR spectra of bare aluminum, aluminum thermally treated at 160 °C for two hours, and aluminum with water adsorbed on the surface; and (**b**) FTIR spectra of aluminum thermally treated at 80 °C/60 s, 120 °C/60 s, and 160 °C/2 h.

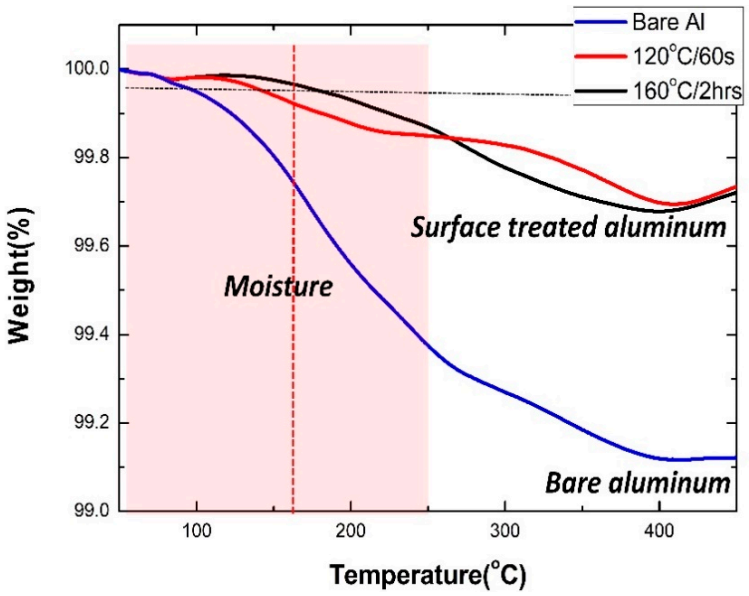

Figure 5. TGA results of bare aluminum and samples thermally treated at 120 °C for 60 s and 160 °C for 2 h after coating with a surface treatment agent.

3.2. Pouch-Film Performance Test

The aluminum surfaces were coated via direct gravure under the above heat treatment conditions, and the samples were dried for 60 s at 120 °C and 60 s at 160 °C. After one sample was dried in the oven for 60 s at 160 °C, additional drying was performed for 2 h. After this, the surface was coated with olefine adhesive and lamination was performed with CPP

film. Three samples were aged for three days at 55 °C, and the adhesive strength between the aluminum and the CPP was examined according to the heat treatment conditions. The adhesive strength was measured using a universal testing machine. During the measurements, water was sprayed on the aluminum and CPP interface to examine the changes in adhesive strength. As shown in Figure 6, the initial strength of the 160 °C/2 h sample is 2400 gf/15 mm. However, the two samples show relatively low initial adhesive strengths under different drying conditions. After water spraying, changes in adhesive strength were observed. However, the adhesive strength of the 160 °C/2 h sample did not decrease after being sprayed with water.

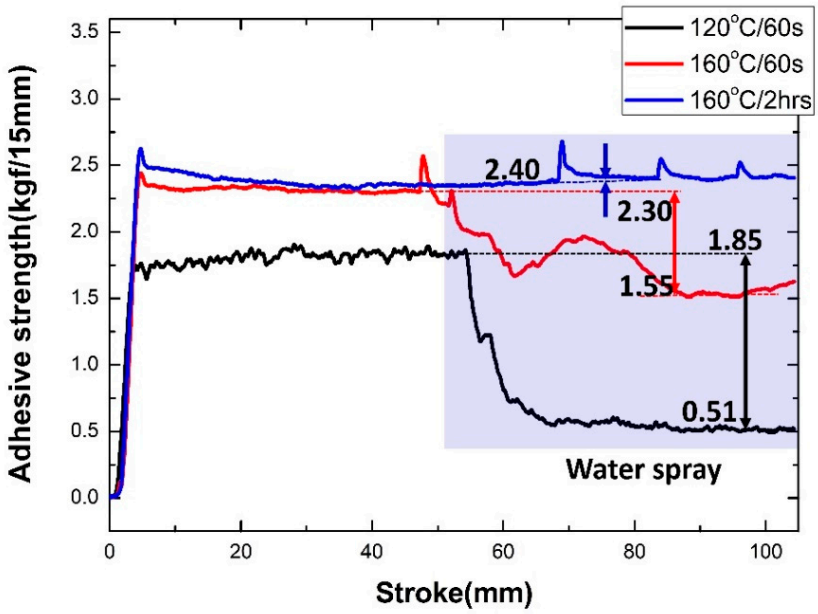

Figure 6. Initial strengths of the pouch samples manufactured after coating with a surface treatment agent and drying at 120 °C for 60 s, 160 °C for 60 s, and 160 °C for 2 h, and changes in adhesive strength after water spraying.

The reductions in adhesive strength became more pronounced as the drying temperature and drying time decreased. If moisture persisted within the coated surface treatment agent due to incomplete drying, as depicted in Figure 7a, the surface-treated layer might not achieve robustness, leading to weak adhesive strength between the adhesive layer and the aluminum. If moisture was added by water spraying, the interface between the aluminum and the adhesive layer was destroyed, and the adhesive strength was reduced. On the contrary, if the sample was sufficiently dried, as in the case of the 160 °C/2 h sample in Figure 7b, the adhesive layer and aluminum adhered to each other sufficiently. Failure of the adhesive layer occurred when aluminum was separated from the CPP film. If water was sprayed into this gap, the adhesive attached to the aluminum surface, leaving no space for the moisture to spread. Consequently, the adhesive strength was not reduced. From the SEM images (Figure 7c,d) of the aluminum surface that were captured after the CPP film was delaminated from the laminated pouch film under 80 °C/60 s and 160 °C/2 h conditions. It can be observed that some of the adhesive layer remains on the aluminum surface of the 80 °C/60 s sample in Figure 7c, whereas the aluminum surface of the 160 °C/2 h sample in Figure 7d is very clean. Figure 7e shows the cross-sectional view of the SEM images of the layers of the aluminum laminated battery cell after bending. The layered structure of the manufactured pouch battery cell in which the aluminum foil is coated in the adhesive with the surface treatment can be clearly observed.

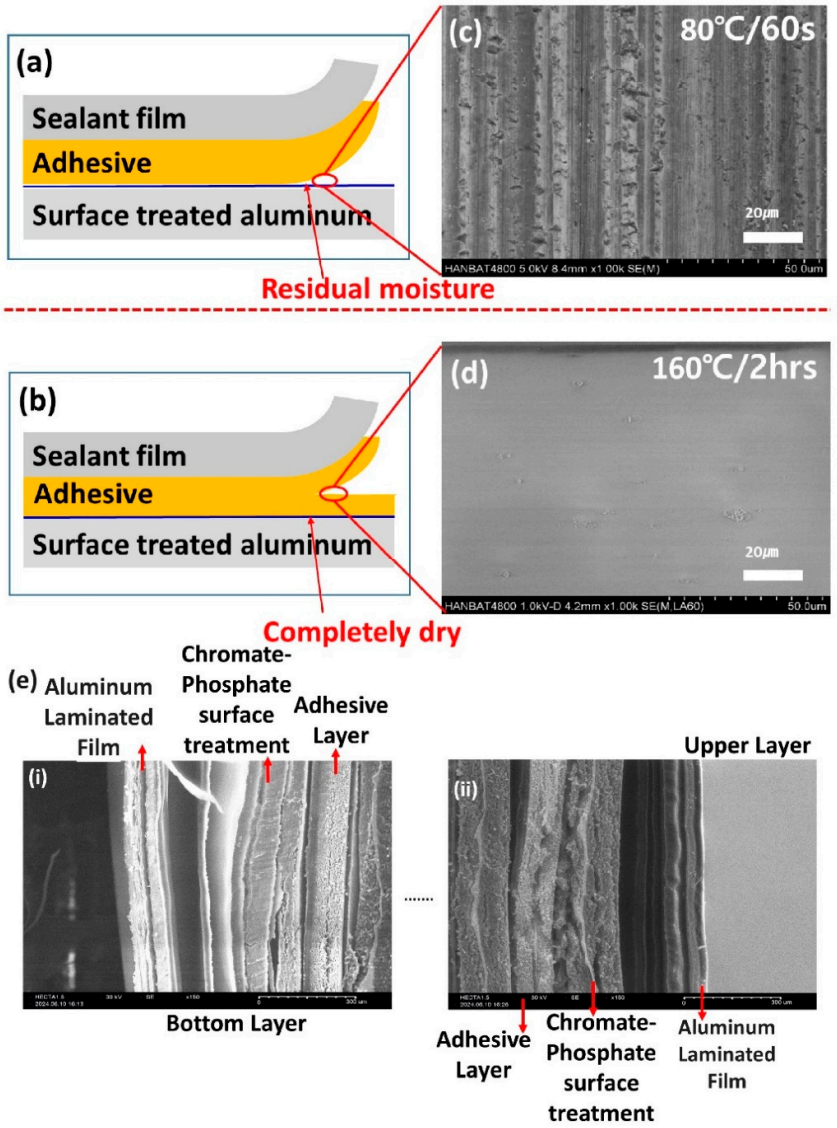

Figure 7. (**a**) Adhesion of aluminum and CPP film; (**c**) status of the aluminum surface, when moisture remains on the surface-treated layer; (**b**) adhesion of aluminum and CPP film; (**d**) SEM image of the aluminum surface after sufficient drying of the surface-treated layer; (**e**) cross-sectional SEM images of the layers after bending. (**i**) Upper layer; and (**ii**) bottom layer.

Pouch specimens manufactured under the three heat-treatment conditions mentioned above were immersed in the electrolyte for one day at 85 °C, and the changes in adhesive strength between the aluminum and the CPP film were examined. Figure 8a shows the chemical resistance results for the three samples. The chemical resistance of the three samples did not vary greatly, but the pouch film that completed 2 h of drying at 160 °C had the highest adhesive strength of 1240 gf/15 mm. Moreover, the resistance of the electrolyte decreased slightly with the reduced drying temperature and time. This occurred because of the generation of hydrofluoric acid as the moisture within the pouch reacted with the organic solvent electrolyte. Hydrofluoric acid corroded the aluminum surface and reduced the adhesive strength between the aluminum and the CPP film. The optimal conditions for chemical and physical bonding between the surface treatment agent and adhesive can easily be seen via the timely changes caused by electrolyte immersion. To perform the electrolyte immersion experiments, similar amounts of urethane, ester, and olefin adhesives were each placed in glass dishes. The electrolyte was added at room temperature to immerse the adhesives, and weight changes were measured for one week. From the first day of the

immersion tests, both the urethane and ester adhesives achieved a significant increase in weight due to the expansion of the electrolyte. The appearance of adhesives changed from the initial hard form to a soft gel form. However, the polymer-type adhesive was in an almost stable state, with no significant weight changes as compared to the other adhesives.

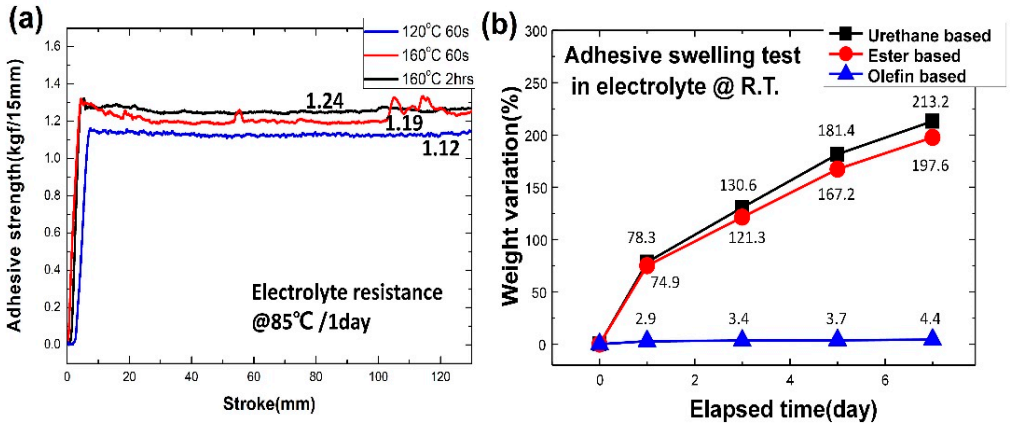

Figure 8. (**a**) Electrolyte resistance results of the pouch samples under 85 °C/1 day condition and different thermal treatment conditions; and (**b**) weight variations in urethane-based, ester-based, and olefin-based adhesives with electrolyte immersion at room temperature.

Figure 8b shows the weight changes due to electrolyte immersion. Both the urethane and ester adhesives exhibit high polarity, and the electrolyte may have dissolved them and entered the spaces between the adhesive molecules.

Figure 9 shows the adhesive strengths of pouch films manufactured using different adhesives after being coated with the surface treatment agent, dried at the optimal drying temperature and time, immersed in the electrolyte at 85 °C, and measured via the 180° delamination tests. The initial adhesive strength of each adhesive was satisfactory, as the aluminum's coating of surface treatment agent was in a stable form; however, the adhesive strength of the urethane and ester adhesives decreased over time after being immersed at 85 °C (green arrow).

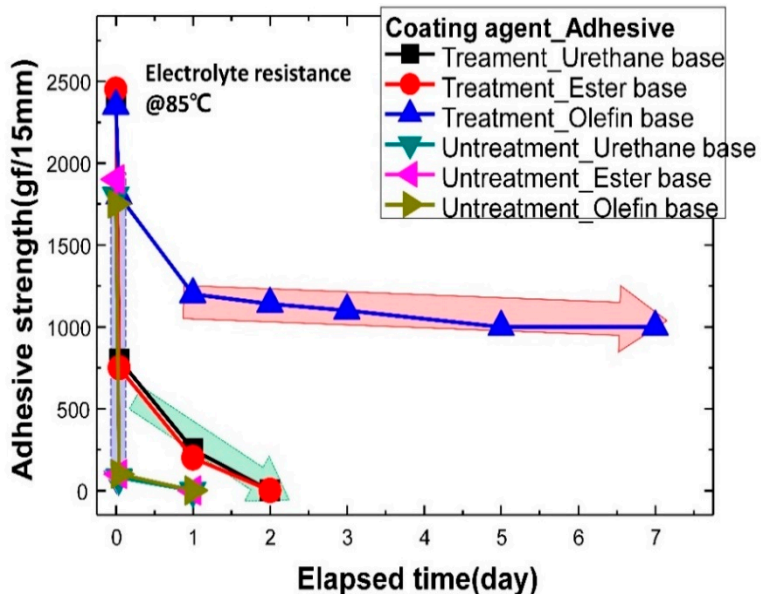

Figure 9. Changes in electrolyte resistance of the pouch films of different adhesives and surface treatment agent in the electrolyte at 85 °C with time.

In contrast, the olefin adhesive maintained high adhesive strength despite the effects of the highly active electrolyte (red arrow). As can be observed in the sealing test results in Figure 8b, the olefin adhesive has strong electrolyte resistance in comparison to the urethane and ester adhesives. The results of these experiments show that the olefin adhesive had an adhesive strength of 1200 gf/15 mm after one day of immersion in the electrolyte at 85 °C. Even after seven days, it maintained a high adhesive strength of 1000 gf/15 mm. In short, the chemical resistance and adhesive strength are determined by the corrosion resistance, compactness, and hydrophilia of the surface treatment agent and the adhesiveness and chemical resistance of the adhesive. In addition, the adhesive strength of untreated aluminum decreased significantly, to 100 gf/15 mm, within one hour at 85 °C, regardless of the adhesive (blue arrow). This suggests that the adhesive's electrolyte resistance and the effect of the surface treatment agent are both important factors that affect the strength of the adhesive. Table 1 below presents the electrolyte resistance results provided in Figure 9.

Table 1. Electrolyte resistance of pouch films fabricated via combinations of various surface treatment agents and adhesives at 85 °C.

Coating Agent Adhesive	Unit	Electrolyte Resistance at 85 °C/day						
		0	0.04 (1 h)	1	2	3	5	7
Urethane	gf/15 mm	2400	800	250	0	_	_	_
Ester		2450	750	200	0	_	_	_
Olefin		2350	1800	1200	1140	1100	1000	1000
Untreatment_Urethane		1800	80	0	_	_	_	_
Untreatment_Ester		1900	100	0	_	_	_	_
Untreatment_Olefin		1750	100	0	_	_	_	_

3.3. Stability Test for Flexible Battery

Figure 10 shows the specifications and appearance of the flexible cells manufactured in a flexible flange form that could be used on curved surfaces such as the headbands in headphones.

Bending tests were performed to examine the flexible cell's performance according to the number of bending cycles. As shown in Figure 11, the tests were performed at curvature radii of R55−R95 in a single direction at a rate of once every two seconds.

Before the bending tests, the cells were conditioned with a 0.2 C 4.35 V CC−CV 0.05 C cut-off charge. Before conducting the tests and performing bending, a measurement device was connected to the cathode tab and aluminum layer in the pouch to measure data for 1.5 s at 50 V.

The AC−IR measurement results confirmed that the change in the electrode's resistance due to bending was approximately 9−10% and the insulation-resistance results confirmed that the cell was in good condition, maintaining a resistance in the order of MΩ even after 3000 bending cycles. The performance changes, according to the number of bending cycles, are presented in Table 2. The resistance change observed in the flexible cell after bending are compared with other reported results and presented in Table 3. In the manufactured flexible pouch cell, the layered structure, combining metal foil (aluminum) and polymer film, distributes stress more effectively. The application of surface treatment agents to the aluminum surface improves the adhesion properties and corrosion resistance. This treatment enhances the bonding between the aluminum and the adhesive, which leads to a stronger connection between the layers. Therefore, the mechanical strength of the overall structure is improved.

(**a**)

Item	Specification		
Materials	Cathode	Contents	LCO Base
		Unit Area Capacity	4.50 mAh/cm²
		Density	3.47 g/cm³
		Total Thickness	110 μm (Foil 16 μm)
		Width × Length	19.1 × 174.5 (mm²)
		Qty	5 pcs
	Anode	Contents	Artificial Graphite Base
		Unit Area Capacity	4.95 mAh/cm²
		N/P ratio	1.10
		Density	1.53 g/cm³
		Total Thickness	126 μm (Foil 8 μm)
		Width × Length	20.6 × 176.5 (mm²)
		Qty	6 pcs
	Separator	Material	PE (20 μm)
	Electrolyte	Contents	LiPF6 Base
	Al Pouch	Thickness	153 μm × 2 Layer
		Sealing Thickness	158 μm (30% ↓ of CPP)
	Tab	Materials	(+): Al, (-): Ni
Cell	Thickness	Before Forming	2.00 mm
		After Forming (for bending)	2.80 mm
	Width × Length		26 × 175 (mm²)
	Capacity		750 mAh

(**b**)

Figure 10. (**a**) Specification table for manufactured flexible cells; and (**b**) fabricated flexible cell.

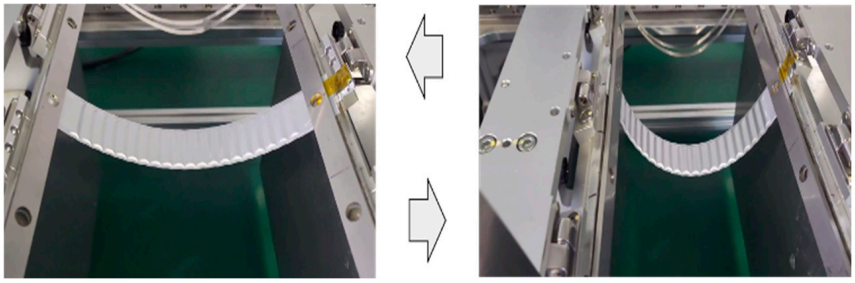

Figure 11. Bending test appearance.

Table 2. Bending test results of flexible cell.

Item		Bending Times			
		0	1000	2000	3000
Sample 1	AC−IR (mΩ)	22.2	23.0	24.2	24.6
	Insulation resistance (MΩ)	>200	>200	>200	141.8
Sample 2	AC−IR (mΩ)	22.0	22.8	23.8	24.0
	Insulation resistance (MΩ)	>200	>200	>200	129.l6

Table 3. Comparison of bending performance of flexible cell.

	Materials	No. of bending	Capacitance retention (%)	References
Bending Properties	Cu film on PI	1000	1.5	[24]
	c-ITO/graphene/PET films	1000	1.12	[25]
	Pyrolyzed BC (p-BC)/polydimethylsiloxane (PDMS) composites	5000	4	[26]
	Pouch cell using LCO Base cathode and Artificial Graphite Base anode	3000	9−10	This work

Figure 12 shows the battery performance before and after bending for both the fabricated flexible cells. The initial capacity of sample1 and sample2 before bending is 774 mAh and 754 mAh, respectively. No significant changes are observed in battery performance after bending. The capacity of sample1 and sample2 after bending is 773 and 750 mAh, respectively. A capacity retention of 99% is revealed after 3000 cycles. Both the samples exhibit a stable voltage over a large capacity range, indicating the healthy performance of the battery cells and highlighting their suitability for flexible electronics devices. Table 4 summarizes the cycling performance of different flexible battery cells after bending. The results demonstrate that the highest capacity retention was observed in this manufactured pouch cell.

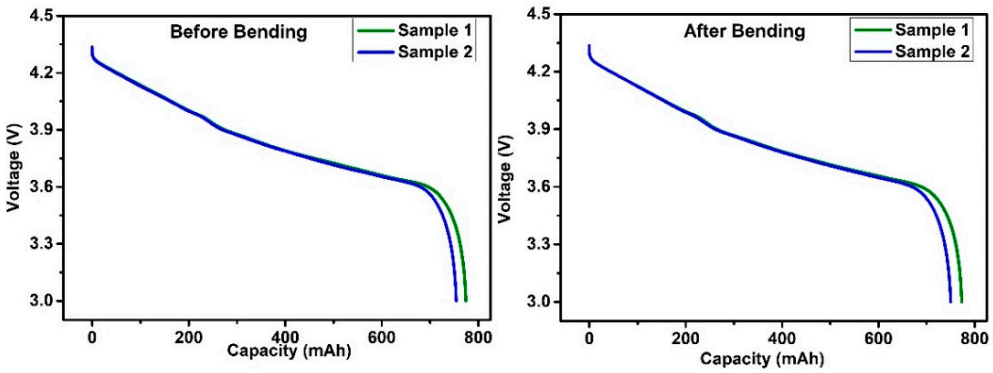

Figure 12. Battery performance before and after bending.

Table 4. Comparison of battery performance of flexible cell.

	Materials	No. of bending	Capacitance retention (%)	References
Bending Performance	Coin cell using LCO as cathode and graphite as anode	2000	92.18	[27]
	MnO_2/CNT as anode and Zn/modified textile as cathode	500	98.5	[28]
	MnO_2/modified textile as anode and Zn/modified textile as cathode	1000	91	[29]
	Pouch cell using LCO Base cathode and Artificial Graphite Base anode	3000	99	This work

4. Conclusions

This study manufactured a pouch film using adhesive materials with surface treatment agents under various time and temperature conditions in order to improve the adhesive strength and chemical resistance of electric vehicle secondary-battery external pouches. The differences in adhesive strength and chemical resistance were examined under different conditions. The experiment results showed a significant difference in the adhesive strength when the aluminum surface was coated with a surface treatment agent, followed by spraying of water on the aluminum and CPP film in the 180° delamination tests. The moisture remained on the surface, reduced the corrosion resistance of the aluminum surface, and the adhesion between aluminum and the adhesive, which led to a reduction in the adhesive strength. In electrolyte-sealing tests with various adhesive materials, the olefin adhesive maintained a relatively stable weight, following electrolyte infiltration into the material, in comparison to the urethane and ester adhesives. In the electrolyte-resistance tests, the pouches were immersed in electrolytes at 85 °C and showed a high adhesive strength over time. According to the results of this study, manufacturing equipment must be optimized to allow for sufficient drying, or a baking process must be incorporated for additional control over residual moisture in order to utilize pouch films in actual battery casings. Further improvements are necessary for olefin adhesives despite their excellent chemical resistance. The manufactured flexible pouch cell with an olefin adhesive exhibited excellent stability, with an electrode resistance change of 9−10% after 3000 bending cycles, confirming its suitability for integration into wearable devices.

Author Contributions: Conceptualization: G.O. and S.P.M.; methodology: G.O. and M.W.; formal analysis: J.P., J.L. and H.P.; investigation: G.O. and S.P.M.; data curation: H.W.C., J.H.S. and H.P.; writing—original draft preparation, G.O. and S.P.M.; writing—review and editing: J.H.S.; supervision: D.S.K.; All authors have read and agreed to the published version of the manuscript.

Funding: This research was supported by the Basic Science Research Program through the National Research Foundation of Korea (NRF) funded by the Ministry of Education (No. 2018R1A6A1A03026005). This research was supported by a research fund from the Hanbat National University.

Data Availability Statement: Data are contained within the article.

Acknowledgments: Authors Gyeongseok Oh and Snigdha Paramita Mantry contributed equally to this work.

Conflicts of Interest: Author Hyeon Woo Cho was employed by the company Amogreentech Co., Ltd. The remaining authors declare that the research was conducted in the absence of any commercial or financial relationships that could be construed as a potential conflict of interest.

References

1. Dunn, B.; Kamath, H.; Tarascon, J.-M. Electrical energy storage for the grid: A battery of choices. *Science* **2011**, *334*, 928–935. [CrossRef] [PubMed]
2. Palacín, M.R. Recent advances in rechargeable battery materials: A chemist's perspective. *Chem. Soc. Rev.* **2009**, *38*, 2565–2575. [CrossRef]
3. Kitada, K.; Murayama, H.; Fukuda, K.; Arai, H.; Uchimoto, Y.; Ogumi, Z.; Matsubara, E. Factors determining the packing-limitation of active materials in the composite electrode of lithium-ion batteries. *J. Power Sources* **2016**, *301*, 11–17. [CrossRef]
4. Tarascon, J.-M.; Armand, M. Issues and challenges facing rechargeable lithium batteries. *Nature* **2001**, *114*, 359–367. [CrossRef] [PubMed]
5. Armand, M.; Tarascon, J.-M. Building better batteries. *Nature* **2008**, *451*, 652–657. [CrossRef] [PubMed]
6. Wang, Y.; Yi, J.; Xia, Y. Recent progress in aqueous lithium-ion batteries. *Adv. Energy Mater.* **2012**, *2*, 830–840. [CrossRef]
7. Saunier, J.; Alloin, F.; Sanchez, J.Y.; Caillon, G. Thin and flexible lithium-ion batteries: Investigation of polymer electrolytes. *J. Power Sources* **2003**, *119–121*, 454–459. [CrossRef]
8. Tebbe, J.L.; Fuerst, T.F.; Musgrave, C.B. Mechanism of hydrofluoric acid formation in ethylene carbonate electrolytes with fluorine salt additives. *J. Power Sources* **2015**, *297*, 427–435. [CrossRef]
9. Kawamura, T.; Okada, S.; Yamaki, J. Decomposition reaction of $LiPF_6$-based electrolytes for lithium ion cells. *J. Power Sources* **2006**, *156*, 547–554. [CrossRef]
10. Heider, U.; Oesten, R.; Jungnitz, M. Challenge in manufacturing electrolyte solutions for lithium and lithium ion batteries quality control and minimizing contamination level. *J. Power Sources* **1999**, *81*, 119–122. [CrossRef]

11. Lux, S.F.; Chevalier, J.; Lucas, I.T.; Kostecki, P. HF formation in $LiPF_6$-based organic carbonate electrolytes. *J. Power Sources* **2013**, *2*, A121–A123. [CrossRef]
12. Yang, H.; Zhuang, G.V.; Ross Philip, N., Jr. Thermal stability of $LiPF_6$ salt and Li-ion battery electrolytes containing $LiPF_6$. *J. Power Sources* **2006**, *161*, 573–579. [CrossRef]
13. Xia, F.; Xu, S.A. Effect of surface pre-treatment on the hydrophilicity and adhesive properties of multilayered laminate used for lithium battery packaging. *Surf. Sci.* **2013**, *268*, 337–342. [CrossRef]
14. Chibowski, S.; Knipa, M. Studies of the influence of polyelectrolyte adsorption on some properties of the electrical double layer of ZrO_2-electrolyte solution interface. *J. Dispersion Sci. Technol.* **2000**, *21*, 761–783. [CrossRef]
15. Niknahad, M.; Moradian, S.; Mirabedini, S.M. The adhesion properties and corrosion performance of differently pretreated epoxy coatings on an aluminium alloy. *Corros. Sci.* **2010**, *52*, 1948–1957. [CrossRef]
16. Shi, C.; Yu, M. Flexible solid-state lithium-sulfur batteries based on structural designs. *Energy Stor. Mater.* **2023**, *57*, 429–459. [CrossRef]
17. Nishide, H.; Oyaizu, K. Toward flexible batteries. *Science* **2008**, *319*, 737–738. [CrossRef] [PubMed]
18. Taberna, P.L.; Mitra, S.; Poizot, P.; Simon, P.; Tarascon, J.M. High rate capabilities Fe_3O_4-based Cu nano-architectured electrodes for lithium-ion battery applications. *Nat. Mater.* **2006**, *5*, 567–573. [CrossRef]
19. Song, H.K.; Palmore, G.T.R. Redox-active polypyrrole: Toward polymer-based batteries. *Adv. Mater.* **2006**, *18*, 1764–1768. [CrossRef]
20. Miller, S.A.; Martin, C.R. Redox modulation of electroosmotic flow in a carbon nanotube membrane. *J. Am. Chem. Soc.* **2004**, *126*, 6226–6227. [CrossRef]
21. Hofmann, A.; Hanemann, T. Novel electrolyte mixtures based on dimethyl sulfone, ethylene carbonate and $LiPF_6$ for lithium-ion batteries. *J. Power Sources* **2015**, *298*, 322–330. [CrossRef]
22. Davis, J.R. *Corrosion of Aluminum and Aluminum Alloys*; ASM International: Almere, The Netherlands, 1999.
23. MeeJoo, S.; Maneeprakorn, W.; Winotai, P. Phase and thermal stability of nanocrystalline hydroxyapatite prepared via microwave heating. *Thermochimica. Acta* **2006**, *447*, 115–120. [CrossRef]
24. Kim, T.W.; Lee, J.S.; Kim, Y.C.; Joo, Y.C.; Kim, B.J. Bending strain and bending fatigue lifetime of flexible metal electrodes on polymer substrates. *Materials* **2019**, *12*, 2490. [CrossRef] [PubMed]
25. Lee, S.J.; Kim, Y.; Hwang, J.Y.; Lee, J.H.; Jung, S.; Park, H.; Cho, S.; Nahm, S.; Yang, W.S.; Kim, H.; et al. Flexible indium–tin oxide crystal on plastic substrates supported by graphene monolayer. *Sci. Rep.* **2017**, *7*, 3131. [CrossRef]
26. Liang, H.W.; Guan, Q.F.; Zhu, Z.; Song, L.T.; Yao, H.B.; Lei, X.; Yu, S.H. Highly conductive and stretchable conductors fabricated from bacterial cellulose. *NPG Asia Mater.* **2012**, *4*, e19. [CrossRef]
27. Meng, Q.; Wu, H.; Mao, L.; Yuan, H.; Ahmad, A.; Wei, Z. Combining electrode flexibility and wave-like device architecture for highly flexible Li-ion batteries. *Adv. Mater. Technol.* **2017**, *2*, 1700032. [CrossRef]
28. Li, H.; Liu, Z.; Liang, G.; Huang, Y.; Huang, Y.; Zhu, M.; Pei, Z.; Xue, Q.; Tang, Z.; Wang, Y.; et al. Waterproof and tailorable elastic rechargeable yarn zinc ion batteries by a cross-linked polyacrylamide electrolyte. *ACS Nano.* **2018**, *12*, 3140–3148. [CrossRef] [PubMed]
29. Zhao, T.; Zhang, G.; Zhou, F.; Zhang, S.; Deng, C. Toward tailorable Zn-ion textile batteries with high energy density and ultrafast capability: Building high-performance textile electrode in 3D hierarchical branched design. *Small* **2018**, *14*, 1802320. [CrossRef]